

# Spectrum of Cosmological Perturbations from Multiple-Stage Inflation

M. Sakellariadou<sup>(a)</sup> and N. Tetradis<sup>(b)</sup>

<sup>(a)</sup> *Département de Physique Théorique, Université de Genève,  
24 quai E. Ansermet, CH-1211 Geneva, Switzerland*

<sup>(b)</sup> *Scuola Normale Superiore, Piazza dei Cavalieri 7, 56100 Pisa, Italy*

## Abstract

Within the context of supersymmetric hybrid inflation, we study a multiple-stage inflationary scenario that can generate a primordial spectrum of adiabatic density perturbations with a break at  $k_b \simeq 0.05 h \text{ Mpc}^{-1}$ . The presence of such a break is supported by the APM galaxy survey data. We consider a specific model within this scenario and confront it with observational data. We reproduce the angular power spectrum of CMB anisotropies, and also account for the break in the power spectrum of galaxy clustering. In addition, we find a value for  $\sigma_8$  in agreement with the one deduced from observations. A characteristic property of the spectrum is a drop of the spectral index from  $n \simeq 1$  to  $n \sim 0.6$  at  $k \sim k_b$ .

PACS number: 98.80.Cq, 98.80.-k, 98.95.D

# 1 Introduction

The origin of the measured anisotropies in the cosmic microwave background and the generation and evolution of large-scale structure in the universe, such as the observed clustering in the galaxy distribution, represent outstanding questions in modern cosmology. Within the framework of gravitational instability, there are two currently investigated families of models to explain the formation of the observed structure. Initial density perturbations can either be due to “freezing in” of quantum fluctuations of a scalar field during an inflationary period [1], or they may be seeded by topological defects, which can form naturally during a symmetry breaking phase transition in the early universe [2]. The cosmic microwave background (CMB) anisotropies provide a link between theoretical predictions and observational data, which may allow us to distinguish between inflationary models and defect scenarios by purely linear analysis [3].

Within the inflationary paradigm, a possible mechanism for the generation of the angular power spectrum of CMB anisotropies and the creation of the large-scale structure is based on the quantum fluctuations that exited the horizon during inflation [4]. These fluctuations are the source of the primordial spectrum of density inhomogeneities [5], which has left an imprint on the CMB. The observed large-scale structure could have been generated by the growth through gravitational instability of this primordial spectrum of perturbations in the otherwise uniform distribution of matter.

By making some assumptions about the matter content of the early universe, one can investigate whether a given spectrum of primordial perturbations can evolve into the large-scale structure observed today. The evolution of the spectrum depends crucially on the nature and amount of the dark matter in the universe. The two extreme cases, of hot dark matter (HDM) and of cold dark matter (CDM), lead to inconsistencies with observational data. The HDM model has been abandoned, since the thermal motion of massive neutrinos wipes out any small-scale structure [6]. On the other hand, the standard CDM model with a flat (spectral index  $n = 1$ ) initial spectrum of adiabatic perturbations predicts too much power on small scales, if one normalizes it to the COBE data at large scales. The standard CDM model leads to a value  $\sigma_8 \simeq 1.2$  for the variance of the total mass fluctuation in a sphere of radius  $8 \text{ Mpc}/h$  [7]. On the other hand, the observational value, inferred from the abundances of rich clusters of galaxies, is  $\sigma_8 \simeq 0.6 \pm 0.2$  [8, 9].

As the standard CDM model is a generally successful model (e.g., it successfully reproduces galaxy clustering statistics, the various epochs of structure formation, as well as peculiar velocity flows, while it maintains CMB anisotropies at a level lower than observational upper limits), several approaches have been proposed, which modify its underlying assumptions (for a review see Ref. [10]). In order to render CDM models compatible with observational data, one possibility is to change the initial spectrum of perturbations by introducing a tilted (spectral index  $n < 1$ ) scale-free spectrum. However, this approach has not led to successful predictions [11]. Another approach is to consider less standard values for the cosmological parameters, while leaving the initial spectral index unchanged (i.e.,  $n \simeq 1$ ). For instance, one can either investigate CDM models with a higher fraction of baryons [12], or models which have a mixture of CDM with an amount of HDM, or even models with a positive cosmological constant [13, 14].

Another interesting possibility is to consider power spectra with a break, which arise naturally in models with more than one stages of inflation – an approach adopted by several authors [15]–[18]. A model of double chaotic inflation which generates such a spectrum has been studied in detail in Refs. [16, 19, 20]. The model contains two scalar fields with disconnected quadratic

potentials.

In this paper, we discuss the possibility of a multiple-stage inflationary scenario within the context of supersymmetric hybrid inflation [21]. The necessary superpotential can arise in supersymmetric GUT models. Moreover, the observable part of inflation takes place for field values below the Planck scale, so that supergravity corrections are under control. Inflationary models such as the one we are considering here have been discussed in Ref. [22], and have been shown to survive the supergravity corrections in Ref. [23].

A strong motivation for these models has its origin in the issue of the initial conditions [24]–[26] that are necessary for hybrid inflation [27]<sup>1</sup>. This is a consequence of the presence of (one or more) scalar fields orthogonal to the inflaton, and the constraint from the COBE data on the inflationary energy scale  $V^{1/4}$  (determined by the vacuum energy density during inflation), which must be at least two or three orders of magnitude smaller than the Planck scale [29]<sup>2</sup>. The difference between the energy scale  $m_{Pl}$  at the end of the Planck era, when classical general relativity becomes applicable, and the inflationary scale  $V^{1/4}$  implies that the various fields evolve for a long time before settling down along the inflationary trajectory. The Hubble parameter  $H$  sets the scale for the “friction” term in the field evolution equations. When the energy density drops much below  $m_{Pl}^4$ , the smallness of this “friction” term results in a very long evolution, during which the fields oscillate around zero many times. Some of the trajectories eventually settle down in the valley of the potential that produces inflation. However, the sensitivity to the initial conditions is high because of the long evolution. A slight variation of the initial field values separates inflationary trajectories from trajectories that lead to the minima of the potential, where inflation does not occur. As a result, the initial field configuration must be extremely fine-tuned for inflation to set in. The fields orthogonal to the inflaton (whose typical fluctuations at the end of the Planck era are  $\sim m_{Pl}$ ) must be zero with an accuracy of at least  $\sim 10^{-5}m_{Pl}$  over regions that exceed the initial Hubble length by one or two orders of magnitude [26].

In Ref. [22] a simple resolution of the issue of fine-tuning described above was suggested. A scenario with two stages of inflation was proposed within the context of global supersymmetry. The first stage has a typical scale  $\sim m_{Pl}$ , which implies that the “friction” term in the field evolution equations of the fields is large. As a result, the system settles down quickly along an almost flat direction of the potential and this stage of inflation occurs naturally. By generating an exponential expansion of the initial region of space, it also provides the homogeneity that is necessary for the second stage. The latter has a characteristic scale much below  $m_{Pl}$  and generates the density perturbations that result in the CMB anisotropy observed by COBE. This scenario was generalized in the context of supergravity in Ref. [23].

It is a logical next step to contemplate the possibility of a multiple-stage inflationary scenario, with a sequence of scales that starts near  $m_{Pl}$  and continues down to the scale implied by COBE, or even to lower energy scales. For inflation driven by one field in the context of supergravity, such a possibility has already been proposed in Ref. [18] and has been associated with a break at  $k_b \simeq 0.05 h \text{ Mpc}^{-1}$  in the power spectrum of galaxy clustering derived from the APM galaxy survey. This break has been linked to a possible phase transition between two of the inflationary stages. In this paper we would like to provide another realization of such a scenario, within a multi-field theory, with an estimation of the predicted power spectrum. The determination of the spectrum during the phase transition is beyond our technical capabilities at the moment. However, the phase transition affects only a small range of scales, while the rest of the power

---

<sup>1</sup>An alternative mechanism for the resolution of this problem has been proposed in Ref. [28].

<sup>2</sup>Throughout the paper we use the “reduced” Planck scale  $m_{Pl} = M_{Pl}/\sqrt{8\pi}$ ,  $M_{Pl} = 1.22 \times 10^{19}$  GeV.

spectrum is strongly constrained by the observational data.

Firstly, we are interested in examining whether the COBE data can be made compatible with the data of galaxy surveys, employing the smallest number of cosmological parameters. More specifically, we consider a CDM model, with zero cosmological constant, present Hubble parameter  $h = 0.5$  ( $H_0 \equiv h$  100 km/s/Mpc) and flat geometry  $\Omega_{matter} = 1$ . We assume that the fraction of the critical density in baryons is  $\Omega_b = 0.05$  and in cold dark matter  $\Omega_{CDM} = 0.95$ . Subsequently, we repeat the calculation, allowing for a non-zero value of the cosmological constant, a scenario supported by recent observations [14].

In Section 2 we discuss the general form of the power spectrum predicted by the APM data. In Section 3 we present our model and in Section 4 the properties of the inflationary stages. The primordial power spectrum in our model is calculated in Section 5 and is compared with observations in Section 6. Our conclusions are given in Section 7.

## 2 The APM power spectrum

An indication for the possibility of more than one stages of inflation is provided by the power spectrum deduced from the APM galaxy survey [30]. This spectrum has a break at a characteristic scale  $k_b \simeq 0.05 h \text{ Mpc}^{-1}$  [31, 32, 18, 33]. One explanation for this break could be a sharp change of the spectral index of the primordial spectrum between two stages of inflation [18]. In this section we summarize the main points of the analysis in the above references, in order to motivate the multiple-stage scenario. In the following sections we shall show how such a scenario can be realized in the context of a specific model.

In Fig. 1 we plot the logarithmic slope of the power spectrum recovered from the APM angular galaxy catalogue [31, 33]. (We have used the data of Table 2 in Ref. [33].) The slope has been calculated through a least-squares fit for groups of 3 data points, assuming that the spectrum is locally linear in a logarithmic scale. The results are in agreement with the detailed analysis of Ref. [33], even though our estimated errors are slightly different. A sharp change in the slope of the spectrum is visible around  $k_b \simeq 0.05 h \text{ Mpc}^{-1}$ .

This break persists even after the effects of the non-linear evolution of matter fluctuations (when the density contrast becomes of order 1) have been removed. Through  $N$ -body simulations, Baugh and Gaztañaga [33] have estimated the linear spectrum that gives rise to the observed spectrum for a spatially flat universe with critical matter density and zero cosmological constant. Their estimate is well fitted by the curve [33, 34]

$$P_l(k) = \frac{Ck^\alpha}{[1 + (k/k_b)^2]^\beta}, \quad (2.1)$$

with  $C \simeq 7.0 \times 10^5$ ,  $k_b \simeq 0.05 h \text{ Mpc}^{-1}$ ,  $\alpha \simeq 1$ ,  $\beta \simeq 1.6$ . This result is in agreement with the spectrum obtained through the application of the formula of Jain *et al.* [35] for the relation between the linear and non-linear spectra. The formula of Peacock and Dodds [36] does not lead to very good agreement with the results of the  $N$ -body simulations [34]. In Fig. 1 we display the logarithmic slope of the linear spectrum as predicted by Eq. (2.1) (solid line). The sharp decrease in the slope is again apparent.

The implications for the primordial spectrum can be obtained if one deconvolutes the spectrum by using the linear transfer function, which determines the scale-dependent growth of linear perturbations. A parametrization of this function is given by the relation [37]

$$T(k) = \left[ 1 + \left\{ ak + (bk)^{3/2} + (ck)^2 \right\}^\nu \right]^{-1/\nu}, \quad (2.2)$$

with  $a = 6.4 \Gamma^{-1} h^{-1} \text{Mpc}$ ,  $b = 3 \Gamma^{-1} h^{-1} \text{Mpc}$ ,  $c = 1.7 \Gamma^{-1} h^{-1} \text{Mpc}$ ,  $\nu = 1.13$  and  $\Gamma = \Omega_b h e^{-2\Omega_b}$ , where  $\Omega_b$  is the fraction of critical density in baryonic matter. For  $h = 0.5$ ,  $\Omega_b = 0.05$ , the spectral index  $n$  of the primordial spectrum  $P(k) \sim P_l(k)/T^2(k)$  is given by the dashed line in Fig. 1. A transition from a value  $n \simeq 1$  at large scales to an average value  $n \sim 0.5$  at small scales is observed. It must be pointed out that the above analysis cannot be considered conclusive, as the parametrization of Eq. (2.2) may not be sufficiently accurate. In section 6 we present a detailed comparison with the linear power spectrum of Eq. (2.1) using the code CMBFAST of Seljak and Zaldarriaga [38].

The variation of the spectral index can be explained by the generation of density perturbations during two stages of inflation, driven by fields with different potentials. The first stage must have lasted long enough for scales between  $k \sim 3 \times 10^{-4} h \text{ Mpc}^{-1}$  (relevant for the COBE data) and  $k \sim k_b \simeq 5 \times 10^{-2} h \text{ Mpc}^{-1}$  to have crossed outside the horizon during its duration. This requires at least 5 e-foldings to be generated by the first stage of inflation. The large deviation of the spectral index from 1 has strong implications for the duration of the second stage. For the models of interest to us, the inflationary potential has the general form  $V \simeq V_0(1 + cf(\phi/m_{Pl}))$ , where  $c$  is a small constant. Moreover, the inflaton field is constrained to be  $\phi \lesssim m_{Pl}$ . A general analysis of the spectral index predicted by such potentials, for various choices of the function  $f(\phi/m_{Pl})$ , is given in Ref. [29]. According to Table 1 of that reference, the total number of e-foldings  $N$  is constrained by the relation  $|n - 1|(N/50) \lesssim 0.08$ . For  $n \simeq 0.6$  we infer  $N \lesssim 8$ . More specifically, for the case  $f(\phi/m_{Pl}) = \ln(\phi/m_{Pl})$  that is relevant for our model,  $|n - 1|(N/50) \simeq 0.02$  and  $N \simeq 2$ .

The above considerations support a picture of multiple short bursts of inflation, with significant variations of the spectral index of the primordial spectrum. The observational data provide information on two of these inflationary stages. The COBE-DMR measurements require a stage with  $n \simeq 1$  and at least 5 e-foldings, while the APM galaxy survey data support the possibility of a second stage with  $n \sim 0.6$  that generates  $\sim 2$  e-foldings. The total number of e-foldings during all the inflationary stages with observable consequences must be  $\sim 60$  for the flatness and horizon problems of standard cosmology to be resolved. However, the stages responsible for the last  $\sim 50$  e-foldings generate density perturbations at scales that are strongly affected by the non-linear evolution. As a result, it is very difficult to extract information on their characteristics.

The above picture contrasts with the double inflationary scenario of Refs. [16, 19, 20], where inflation is driven by two disconnected quadratic potentials for the fields  $\sigma_1, \sigma_2$ . The first stage of inflation occurs for  $\sigma_{1,2} \gg m_{Pl}$  and terminates when  $\sigma_1 \sim m_{Pl}$ , while the second one terminates when  $\sigma_2 \sim m_{Pl}$ . For the second stage to generate less than  $\sim 60$  e-foldings, so that the break in the spectrum is observable, the value of  $\sigma_2$  at its beginning must not be very far from  $m_{Pl}$ . In our model there is no need for a similar adjustment. The requirement of a spectral index significantly below 1 for the part of the spectrum generated by the second stage of inflation automatically constrains the number of e-foldings from this stage to be less than 60, independently of the value of  $\sigma_2$ .

In the following section we describe a model which provides the potential for the two stages of inflation that are relevant for the COBE and APM data.

### 3 The model

The model we consider is described by the superpotential

$$W = S_1 \left( -\mu_1^2 + \lambda_1 \bar{\Phi}_1 \Phi_1 + g \bar{\Phi}_2 \Phi_2 \right) + S_2 \left( -\mu_2^2 + \lambda_2 \bar{\Phi}_2 \Phi_2 \right). \quad (3.1)$$

The superfields  $\Phi_1, \bar{\Phi}_1$  and  $\Phi_2, \bar{\Phi}_2$  transform under internal gauge symmetry groups  $\mathcal{M}_1$  and  $\mathcal{M}_2$  respectively. The  $S_1, S_2$  superfields are gauge singlets. We have assumed that  $S_2$  is the linear combination of gauge singlets that does not couple to  $\bar{\Phi}_1 \Phi_1$  [22]. We make the simplifying assumption that the scalar components of the various superfields are real. The imaginary components do not alter the qualitative picture of inflation in this model, while they would make the calculation of the spectrum of density perturbations much more complicated. Staying along the  $D$ -flat directions, we define canonically normalized scalar fields according to <sup>3</sup>

$$\begin{aligned} S_1 &= \frac{\sigma_1}{\sqrt{2}}, & \Phi_1 &= \bar{\Phi}_1 = \frac{\phi_1}{2}, \\ S_2 &= \frac{\sigma_2}{\sqrt{2}}, & \Phi_2 &= \bar{\Phi}_2 = \frac{\phi_2}{2}. \end{aligned} \quad (3.2)$$

The potential is then given by the expression

$$\begin{aligned} V(\sigma_1, \sigma_2, \phi_1, \phi_2) &= \sum_i \left| \frac{\partial W}{\partial \Phi_i} \right|^2 = \left( \mu_1^2 - \frac{\lambda_1}{4} \phi_1^2 \right)^2 - \frac{g}{2} \mu_1^2 \phi_2^2 + \frac{g^2}{16} \phi_2^4 + \frac{g \lambda_1}{8} \phi_1^2 \phi_2^2 + \frac{\lambda_1^2}{4} \sigma_1^2 \phi_1^2 \\ &\quad + \left( \mu_2^2 - \frac{\lambda_2}{4} \phi_2^2 \right)^2 + \frac{1}{4} (g \sigma_1 + \lambda_2 \sigma_2)^2 \phi_2^2, \end{aligned} \quad (3.3)$$

where the mass scales  $\mu_1, \mu_2$  are chosen  $\mu_1 > \mu_2$ . The minima of this potential are located at

$$\sigma_1 = \sigma_2 = 0, \quad \phi_1^2 = \frac{4}{\lambda_1} \mu_1^2 - \frac{4g}{\lambda_1 \lambda_2} \mu_2^2, \quad \phi_2^2 = \frac{4}{\lambda_2} \mu_2^2. \quad (3.4)$$

For  $\phi_1 = \phi_2 = 0$  the potential is independent of  $\sigma_{1,2}$ . Its value  $V = \mu_1^4 + \mu_2^4$  gives the vacuum energy density during the first stage of inflation. Along this direction, the mass terms of the  $\phi_{1,2}$  fields are

$$M_{\phi_1}^2 = -\lambda_1 \mu_1^2 + \frac{\lambda_1^2}{2} \sigma_1^2, \quad (3.5)$$

$$M_{\phi_2}^2 = -\lambda_2 \mu_2^2 - g \mu_1^2 + \frac{1}{2} (g \sigma_1 + \lambda_2 \sigma_2)^2. \quad (3.6)$$

The mass term  $M_{\phi_1}^2$  becomes negative for

$$\sigma_1^2 < \sigma_{1ins}^2 = \frac{2\mu_1^2}{\lambda_1}. \quad (3.7)$$

This indicates the presence of an instability which can lead to the growth of the  $\phi_1$  field.

---

<sup>3</sup> We use the same notation for the superfields and their scalar components.

Another flat direction (independent of  $\sigma_2$ ) exists for  $\sigma_1 = 0$ ,  $\phi_1^2 = 4\mu_1^2/\lambda_1$ ,  $\phi_2 = 0$ . The value of the potential  $V = \mu_2^4$  gives the vacuum energy density during the second stage of inflation. The mass term of the  $\phi_2$  field is given by

$$M_{\phi_2}^2 = -\lambda_2\mu_2^2 + \frac{\lambda_2^2}{2}\sigma_2^2. \quad (3.8)$$

An instability appears for

$$\sigma_2^2 < \sigma_{2ins}^2 = \frac{2\mu_2^2}{\lambda_2}, \quad (3.9)$$

which can lead to the growth of the  $\phi_2$  field.

The flatness of the potential is lifted by radiative corrections. During the first stage of inflation and for  $\sigma_{1,2}$  far above the instability points, the one-loop contribution to the effective potential is <sup>4</sup>

$$\begin{aligned} \Delta V(\sigma_1, \sigma_2) \simeq & \frac{M_1}{16\pi^2} \lambda_1^2 \mu_1^4 \left[ \ln \left( \frac{\lambda_1^2 \sigma_1^2}{2\Lambda_1^2} \right) + \frac{3}{2} \right] \\ & + \frac{M_2}{16\pi^2} (\lambda_2 \mu_2^2 + g \mu_1^2)^2 \left[ \ln \left( \frac{(g\sigma_1 + \lambda_2 \sigma_2)^2}{2\Lambda_2^2} \right) + \frac{3}{2} \right], \end{aligned} \quad (3.10)$$

where  $M_{1,2}$  are the dimensionalities of the representations of the groups  $\mathcal{M}_{1,2}$  to which the superfields  $\Phi_{1,2}$  belong. The exact value of the normalization scales  $\Lambda_{1,2}$  is not important for our discussion. In the following we shall consider theories in which the two sectors  $(S_1, \Phi_1)$  and  $(S_2, \Phi_2)$  are essentially decoupled. For this reason we shall assume that the coupling  $g$  is sufficiently small for the radiative correction of Eq. (3.10) to be approximated as

$$\Delta V(\sigma_1, \sigma_2) \simeq \frac{M_1}{16\pi^2} \lambda_1^2 \mu_1^4 \left[ \ln \left( \frac{\lambda_1^2 \sigma_1^2}{2\Lambda_1^2} \right) + \frac{3}{2} \right] + \frac{M_2}{16\pi^2} (\lambda_2 \mu_2^2 + g \mu_1^2)^2 \left[ \ln \left( \frac{\lambda_2^2 \sigma_2^2}{2\Lambda_2^2} \right) + \frac{3}{2} \right]. \quad (3.11)$$

The above contribution provides the slope that leads to the slow rolling of the  $\sigma_{1,2}$  fields during the first stage of inflation.

During the second stage of inflation the slope for the  $\sigma_2$  field is provided by the radiative correction

$$\Delta V(\sigma_1, \sigma_2) \simeq \frac{M_2}{16\pi^2} \lambda_2^2 \mu_2^4 \left[ \ln \left( \frac{\lambda_2^2 \sigma_2^2}{2\Lambda_1^2} \right) + \frac{3}{2} \right]. \quad (3.12)$$

Away from the flat directions the radiative corrections are small and we neglect them.

An important question concerns the supergravity corrections to the above potential. In particular, it is important that the flat directions of the potential are not lifted by these corrections [21]. A detailed analysis of this problem is presented in Ref. [23], where it is shown that, for the flat directions to be preserved, at least one of the two inflationary stages must be driven by  $D$ -term energy density [39]. However, the form of the potential is the same as the one we described above. Two flat directions exist with a small slope generated by logarithmic radiative corrections.

---

<sup>4</sup> It must be pointed out that the supersymmetric cancellations that lead to Eqs. (3.10), (3.12) require the inclusion of radiative corrections from both the real and imaginary scalar components of the superfields  $\Phi_1, \Phi_2$ . However, this is the only effect of the imaginary components on the inflationary stages. This is the reason why we omitted them in Eq. (3.3). For a discussion that includes these components see Ref. [22].

## 4 The inflationary stages

The model we described in the previous section allows for two stages of inflation separated by an intermediate stage.

### 4.1 The first stage of inflation

The Hubble parameter during the first stage of inflation is almost constant

$$H_1^2 \simeq \frac{\mu_1^4 + \mu_2^4}{3m_{Pl}^2}. \quad (4.1)$$

We assume that the part of this stage with observable consequences starts at a time  $t_{1i}$  and finishes at a time  $t_{1f}$ . Because of our assumption  $\mu_1 > \mu_2$ , the vacuum energy density associated with the fields  $\sigma_1, \phi_1$  dominates the first stage. Therefore, this stage terminates when the ‘‘slow-roll’’ conditions for  $\sigma_1$  are not satisfied any more. For the potential of Eqs. (3.3), (3.11), this happens for

$$\sigma_1^2(t_{1f}) \equiv \sigma_{1f}^2 \simeq \frac{M_1 \lambda_1^2}{8\pi^2} m_{Pl}^2. \quad (4.2)$$

Unless the coupling  $\lambda_1$  is taken much smaller than 1,  $\sigma_{1f}^2$  is much larger than the instability point  $\sigma_{1ins}^2$  of Eq. (3.7).

The number of e-foldings from a time  $t$  until the end of the first stage is given by

$$N_1(t) = \ln \left( \frac{a_{1f}}{a(t)} \right) = \frac{4\pi^2}{M_1 \lambda_1^2} \frac{\mu_1^4 + \mu_2^4}{\mu_1^4} \frac{\sigma_1^2(t) - \sigma_{1f}^2}{m_{Pl}^2}, \quad (4.3)$$

where  $a(t)$  is the scale factor and  $a_{1f} \equiv a(t_{1f})$ . The total number of e-foldings during the observable part of this stage is given by

$$N_{1tot} = \ln \left( \frac{a_{1f}}{a_{1i}} \right) = \frac{4\pi^2}{M_1 \lambda_1^2} \frac{\mu_1^4 + \mu_2^4}{\mu_1^4} \frac{\sigma_{1i}^2 - \sigma_{1f}^2}{m_{Pl}^2}, \quad (4.4)$$

with  $\sigma_{1i}^2 \equiv \sigma_1^2(t_{1i})$ ,  $a_{1i} \equiv a(t_{1i})$ . The relative change of the values of the two fields during the first stage is

$$\frac{\sigma_2^2(t_{1i}) - \sigma_2^2(t_{1f})}{\sigma_1^2(t_{1i}) - \sigma_1^2(t_{1f})} = \frac{\sigma_2^2(t_{1i}) - \sigma_2^2(t_{1f})}{\sigma_{1i}^2 - \sigma_{1f}^2} = \frac{M_2}{M_1} \frac{(\lambda_2 \mu_2^2 + g \mu_1^2)^2}{\lambda_1^2 \mu_1^4}. \quad (4.5)$$

In the following, we shall use parameters that make this ratio much smaller than 1, so that the evolution of  $\sigma_2$  can be neglected during the first stage of inflation.

### 4.2 The intermediate stage

The intermediate stage lasts between times  $t_{1f}$  and  $t_{2i}$ . After the end of the slow-roll regime, the  $\sigma_1$  field quickly rolls beyond the instability point of Eq. (3.7). Subsequently, large domains start appearing in which the value of the  $\phi_1$  field grows exponentially with time. For statistical systems, for which the expansion of the universe is not relevant, this process is characterized as spinodal decomposition. The expansion of the universe complicates the above picture, but the details are not important for our discussion. We assume that this initial stage of instability is fast, and soon the fields take values away from the  $\sigma_1$  axis and in the vicinity of the minimum

at  $\sigma_1 = 0$ ,  $\phi_1^2 = 4\mu_1^2/\lambda_1$ , where the curvature of the potential is positive. Our assumption is reasonable because the  $\sigma_1$  field rolls to the origin within a time  $\sim H_1^{-1} \simeq \sqrt{3}m_{Pl}/\sqrt{\mu_1^4 + \mu_2^4}$  or slightly larger. On the other hand, the typical time scale for the growth of the  $\phi_1$  field is given by the absolute value of the curvature at the origin and is  $\sim (\sqrt{\lambda_1}\mu_1)^{-1}$ . As a result, we expect that  $\phi_1$  grows to a value near the minimum within a fraction of a Hubble time.

After a short complicated evolution, the massive fields  $\sigma_1$ ,  $\phi_1$  settle into a regular oscillatory pattern around the minimum, with the universe characterized by an equation of state  $p = w\rho$ . For a system of massive oscillating fields, such as the one we are considering,  $w = 0$ . From this point on, the energy density of the oscillating fields is dissipated through the expansion of the universe. If the fields have decay channels into lighter species that eventually thermalize, the equation of state of the radiation-dominated universe has  $w = 1/3$ . When the energy density becomes comparable to  $\mu_2^4$  the second stage of inflation can begin. During the intermediate stage, the scale factor increases by a total amount

$$N_{int} = \ln \left( \frac{a_{2i}}{a_{1f}} \right) = \frac{2}{3(1+w)} \ln \left( \frac{H_1}{H_2} \right), \quad (4.6)$$

where  $a_{2i} \equiv a(t_{2i})$ .

The effect of the oscillations of  $\sigma_1$ ,  $\phi_1$  on the stability of  $\sigma_2$ ,  $\phi_2$  is minimized if the former have fast decay channels into lighter species. Under this assumption, the fields  $\sigma_2$ ,  $\phi_2$  remain constant during the intermediate stage, even when the supergravity corrections are taken into account [23]. In the following we make this assumption and use  $w = 1/3$  during the whole intermediate stage.

### 4.3 The second stage of inflation

This stage starts at a time  $t_{2i}$  and finishes at a time  $t_{2f}$ . The Hubble parameter is

$$H_2^2 \simeq \frac{\mu_2^4}{3m_{Pl}^2}. \quad (4.7)$$

Inflation stops when the ‘‘slow-roll’’ conditions for  $\sigma_2$  are not satisfied any more. For the potential of Eqs. (3.3), (3.12), this happens for

$$\sigma_2^2(t_{2f}) \equiv \sigma_{2f}^2 \simeq \frac{M_2\lambda_2^2}{8\pi^2} m_{Pl}^2. \quad (4.8)$$

Unless the coupling  $\lambda_2$  is taken much smaller than 1,  $\sigma_{2f}^2$  is much larger than the instability point  $\sigma_{2ins}^2$  of Eq. (3.7).

The number of e-foldings from a time  $t$  until the end of the second stage is given by

$$N_2(t) = \ln \left( \frac{a_{2f}}{a(t)} \right) = \frac{4\pi^2}{M_2\lambda_2^2} \frac{\sigma_2^2(t) - \sigma_{2f}^2}{m_{Pl}^2}, \quad (4.9)$$

where  $a_{2f} \equiv a(t_{2f})$ . The total number of e-foldings during this stage is given by

$$N_{2tot} = \ln \left( \frac{a_{2f}}{a_{2i}} \right) = \frac{4\pi^2}{M_2\lambda_2^2} \frac{\sigma_{2i}^2 - \sigma_{2f}^2}{m_{Pl}^2}, \quad (4.10)$$

with  $\sigma_{2i}^2 \equiv \sigma_2^2(t_{2i})$ .

In the next sections we shall consider parameters for which the above equation predicts  $N_{2tot} \simeq 2$  e-foldings. As the accuracy of the analytical expressions presented in this section is questionable for so small  $N_{2tot}$ , we have verified the properties of the second inflationary stage numerically. We have found a value for  $N_{2tot}$  that is close to 3 for our choice of parameters.

#### 4.4 The remaining stages of inflation

The total number of e-foldings during all the inflationary stages with observable consequences must be  $\sim 60$  for the flatness and horizon problems of standard cosmology to be resolved. This means that additional inflationary stages must take place after the first two that we discussed above.

A simple extension of our model that would provide this possibility involves an additional term  $S_3(-\mu_3^2 + \lambda_3 \bar{\Phi}_3 \Phi_3)$  in the superpotential. We assume that the new system of superfields  $S_3, \bar{\Phi}_3, \Phi_3$  is decoupled from the ones driving the first two stages of inflation. The potential and the properties of the third inflationary stage are completely analogous to the ones we described above. For a sufficiently small scale  $\mu_3$  the discussion of the previous subsections is not affected. A third stage of inflation starts after a second intermediate stage, as soon as the energy density becomes comparable to  $\mu_3^4$ . The total number of e-foldings during the third stage is

$$N_{3tot} = \ln \left( \frac{a_{3f}}{a_{3i}} \right) = \frac{4\pi^2}{M_3 \lambda_3^2} \frac{\sigma_{3i}^2 - \sigma_{3f}^2}{m_{Pl}^2}, \quad (4.11)$$

where  $\sigma_{3f}^2/m_{Pl}^2 \simeq M_3 \lambda_3^2/8\pi^2$  and the various quantities are defined in analogy to the first two stages. One can envisage several stages driven by such systems of superfields. The calculation of the supergravity corrections to the potential of such complicated systems of fields is a difficult task. However, we assume that it is possible to guarantee the presence of the necessary number of flat directions, even when supergravity corrections are taken into account.

There are other possible sources of inflation as well. The increase of temperature during the reheating after the first inflationary stages may lead to the restoration of spontaneously broken symmetries. Additional stages of inflation may take place when the temperature falls below the energy scale associated with these symmetries. Inflationary stages, such as the thermal inflation of Ref. [40], may occur even as low as at the TeV scale.

## 5 The primordial spectrum

The primordial spectrum of density inhomogeneities has its origin in the quantum fluctuations that crossed outside the horizon during inflation [4]. The scale  $k$  crosses the Hubble radius when  $k = aH$ . The scale  $k_{COBE}/a_0 \sim H_0$  exited the horizon at the beginning of the observable part of the first stage of inflation. This implies that  $a_0 H_0 = a_{1i} H_1$ . (Here  $a_0, H_0 \simeq (3000 \text{ Mpc})^{-1} h$  are the present values of the scale factor and the Hubble parameter. Following the standard convention, we set  $a_0 = 1$  in the following.)

For  $k \lesssim k_2 = a_{2i} H_2$  the Hubble radius is crossed only once, during the first stage of inflation, while for  $k \gtrsim k_1 = a_{1f} H_1$  it is crossed once during the second stage. The scales  $k_2 < k < k_1$ , however, cross the Hubble radius three times: They exit the horizon during the first stage, re-enter during the intermediate stage and exit again during the second stage. We define the scale  $K$  according to

$$K = \sqrt{k_1 k_2} \quad (5.1)$$

and we obtain

$$\ln\left(\frac{K}{H_0}\right) = N_{1tot} + \frac{1}{2}N_{int} + \frac{1}{2}\ln\left(\frac{H_2}{H_1}\right), \quad (5.2)$$

with  $N_{1tot}$ ,  $N_{int}$  given by Eqs. (4.4), (4.6) respectively. For the ratio  $k_2/k_1$  we obtain

$$\ln\left(\frac{k_2}{k_1}\right) = \left(1 - \frac{2}{3(1+w)}\right)\ln\left(\frac{H_2}{H_1}\right). \quad (5.3)$$

The gravitational potential for scalar metric perturbations that are generated during the first stage of inflation is given by the expression [16, 41, 42]

$$\Phi = 2C\frac{\dot{H}}{H^2} + D\frac{1}{H}\frac{V_1\dot{V}_2 - \dot{V}_1V_2}{2m_{Pl}^2(V_1 + V_2)}, \quad (5.4)$$

with

$$C = -\frac{1}{2}\left[H\left(\frac{V_1}{V_1 + V_2}\frac{\delta\sigma_1}{\dot{\sigma}_1} + \frac{V_2}{V_1 + V_2}\frac{\delta\sigma_2}{\dot{\sigma}_2}\right)\right]_{k=aH} \quad (5.5)$$

$$D = \left[\frac{1}{3H}\left(\frac{\delta\sigma_1}{\dot{\sigma}_1} - \frac{\delta\sigma_2}{\dot{\sigma}_2}\right)\right]_{k=aH}. \quad (5.6)$$

The first term in the right-hand side of Eq. (5.4) can be interpreted as the adiabatic contribution to the spectrum, while the second one corresponds to entropic fluctuations. Until the end of the first stage of inflation (when  $t_1 \simeq t_{1f}$  according to Eq. (4.2)), the functions  $V_1(\sigma_1)$ ,  $V_2(\sigma_2)$  are the potentials of the two disconnected fields  $\sigma_1$ ,  $\sigma_2$  and can be derived from Eqs. (3.3), (3.11):

$$\begin{aligned} V_1(\sigma_1) &= \mu_1^4 + \frac{M_1}{16\pi^2}\lambda_1^2\mu_1^4\left[\ln\left(\frac{\lambda_1^2\sigma_1^2}{2\Lambda_1^2}\right) + \frac{3}{2}\right], \\ V_2(\sigma_2) &= \mu_2^4 + \frac{M_2}{16\pi^2}\left(\lambda_2\mu_2^2 + g\mu_1^2\right)^2\left[\ln\left(\frac{\lambda_2^2\sigma_2^2}{2\Lambda_2^2}\right) + \frac{3}{2}\right]. \end{aligned} \quad (5.7)$$

However, the subsequent evolution of the entropic contribution is very complicated, due to the growth of the  $\phi_1$  field and the possible decay of  $\sigma_1$ ,  $\phi_1$  into lighter species. For this reason, we concentrate on the adiabatic contribution, which can be followed until today. We point out, however, that for our choice of parameters of the model, the total spectrum of adiabatic perturbations is dominated by the fluctuations of the  $\sigma_2$  field, with the contribution of  $\sigma_1$  being negligible (see below). Since the entropic contribution arises because of the simultaneous fluctuations of at least two fields, the dominance of the  $\sigma_2$  fluctuations indicates that the entropic contribution to the spectrum might be subleading.

Assuming that the field fluctuations are random gaussian variables, we obtain for the spectrum of adiabatic density perturbations

$$\delta_H^2(k) = \frac{1}{25\pi^2}\left[\frac{H^2}{m_{Pl}^4}\left\{\left(\frac{V_1}{V_1'}\right)^2 + \left(\frac{V_2}{V_2'}\right)^2\right\}\right]_{k=aH}, \quad (5.8)$$

where primes on  $V_1(\sigma_1)$ ,  $V_2(\sigma_2)$  denote derivatives with respect to  $\sigma_1$ ,  $\sigma_2$  respectively. We assume that the evolution of  $\sigma_2$  is negligible during the first stage of inflation (so that  $\sigma_2 \simeq \sigma_{2i}$  during this whole stage). This is guaranteed if the ratio of Eq. (4.5) is much smaller than 1.

We also concentrate on the case  $V_1/V_1' \ll V_2/V_2'$ , for which the metric perturbations are mainly generated by the fluctuations of the  $\sigma_2$  field during both stages of inflation. This requires

$$\frac{\sigma_{1i}}{M_1} \frac{1}{\lambda_1^2} \ll \frac{\sigma_{2i}}{M_2} \left( \frac{\mu_2^2}{\lambda_2 \mu_2^2 + g \mu_1^2} \right)^2 \quad (5.9)$$

and leads to

$$\delta_H(k) \simeq \frac{8\pi}{5M_2} \left( \frac{\mu_2^2}{\lambda_2 \mu_2^2 + g \mu_1^2} \right)^2 \frac{H_1 \sigma_{2i}}{m_{Pl}^2}. \quad (5.10)$$

The predicted spectrum is scale invariant with a spectral index  $n = 1$  to a very good accuracy. It provides a good approximation to the primordial spectrum for  $k < k_2$ . It should be contrasted with the spectrum predicted by the model of Refs. [16, 19, 20], which has a logarithmic dependence  $\propto \ln^{1/2}(K/k)$  for small  $k$ .

During the second stage of inflation the metric perturbations are generated by the  $\sigma_2$  field and the spectrum is

$$\delta_H(k) \simeq \frac{8\pi}{5M_2 \lambda_2^2} \frac{H_2 [\sigma_2]_{k=aH_2}}{m_{Pl}^2}. \quad (5.11)$$

The field  $\sigma_2$  evolves from  $\sigma_{2i}$  to  $\sigma_{2f}$  during this stage and the resulting spectrum has a spectral index different from 1. The scale dependence is given by the relation

$$\left[ \frac{\sigma_2}{m_{Pl}} \right]_{k=aH_2}^2 = \frac{\sigma_{2i}^2}{m_{Pl}^2} + \frac{M_2 \lambda_2^2}{4\pi^2} \left[ N_{1tot} + N_{int} - \ln \left( \frac{k}{H_0} \right) - \ln \left( \frac{H_1}{H_2} \right) \right]. \quad (5.12)$$

The resulting spectral index is

$$n - 1 = \frac{d \ln \delta_H^2}{d \ln k} = - \frac{M_2 \lambda_2^2}{4\pi^2} \frac{m_{Pl}^2}{\sigma_2^2(k)}, \quad (5.13)$$

with  $\sigma_2(k)$  given by Eq. (5.12). We are interested in scales that crossed outside the horizon during the beginning of the second stage of inflation. For them the spectral index is given by the above expression with  $\sigma_2(k) \simeq \sigma_{2i}$ .

The calculation of the form of the spectrum for scales  $k_2 < k < k_1$  that re-enter the horizon during the intermediate stage is prohibited by the extremely complicated nature of this stage. This is due to the presence of two massive oscillating and decaying fields ( $\sigma_1, \phi_1$ ). However, we do not expect any strong features (such as spikes [43]) in the spectrum associated with the intermediate stage. The situation is very similar to the ‘‘double inflation with a break’’ of Ref. [16]. In that case there is only one massive oscillating field with no decay channels, whose energy is dissipated through expansion. The detailed calculation of the spectrum has not revealed any strong features. In our model, no ‘‘massless’’ fields exist during the inflationary stages, other than  $\sigma_1, \sigma_2$  whose contribution to the spectrum we have computed. The first stage of inflation ends for  $\sigma_1 \sim \sigma_{1f} \gg \sigma_{1ins}$ , long before the orthogonal field  $\phi_1$  becomes massless or develops an instability; and similarly for the second stage. A smooth interpolation between the two parts of the spectrum that we have computed is likely, such as the one indicated by the data.

We also mention that the gravitational wave contribution to the spectrum is not expected to be large. For our choice of the parameters of the model (see next section), it is more than two orders of magnitude smaller than the scalar contribution during the second stage of inflation.

Due to the similarity of the potentials of the first and second stage, we expect that the same is true for the first stage of inflation as well.

Finally, we consider the effect of the subsequent inflationary stages on the spectrum. The presence of a third stage, generated by an additional term  $S_3(-\mu_3^2 + \lambda_3\bar{\Phi}_3\Phi_3)$  in the superpotential, could affect our previous discussion. In order to be more specific, let us concentrate on the second and third inflationary stages. In the presence of additional superfields  $\Phi_3, \bar{\Phi}_3$ , the superpotential associated with the second inflationary stage has the more general form  $S_2(-\mu_2^2 + \lambda_2\bar{\Phi}_2\Phi_2 + g'\bar{\Phi}_3\Phi_3)$ . For sufficiently small coupling  $g'$ , the potential that generates a slope along the flat direction during the second stage has a form analogous to eq. (3.11), i.e.

$$\Delta V(\sigma_2, \sigma_3) \simeq \frac{M_2}{16\pi^2} \lambda_2^2 \mu_2^4 \left[ \ln \left( \frac{\lambda_2^2 \sigma_2^2}{2\Lambda_2^2} \right) + \frac{3}{2} \right] + \frac{M_3}{16\pi^2} (\lambda_3 \mu_3^2 + g' \mu_2^2)^2 \left[ \ln \left( \frac{\lambda_3^2 \sigma_3^2}{2\Lambda_3^2} \right) + \frac{3}{2} \right]. \quad (5.14)$$

For simplicity we assume that the value of  $\sigma_3$  does not change substantially during the second stage. This is expected to be the case for  $\mu_2$  sufficiently larger than  $\mu_3$ . The contribution of the fluctuations of the  $\sigma_3$  field to the spectrum generated during the second stage can be estimated through the analogous of eq. (5.8). These fluctuations do not affect the spectrum if

$$f^2/c^4 \ll 1, \quad (5.15)$$

where

$$f = \frac{\sigma_{3i}}{M_3 \lambda_3^2} \frac{M_2 \lambda_2^2}{\sigma_{2i}},$$

$$c = 1 + \frac{g' \mu_2^2}{\lambda_3 \mu_3^2}. \quad (5.16)$$

The above constraint has implications for the total number of e-foldings  $N_{3tot}$ , given by Eq. (4.11), that can be generated during the third stage. For  $\sigma_{2f} \ll \sigma_{2i}, \sigma_{3f} \ll \sigma_{3i}$ , we can express  $N_{3tot}$  as

$$N_{3tot} = N_{2tot} f \frac{\sigma_{3i}}{\sigma_{2i}}. \quad (5.17)$$

Large values of  $N_{3tot}$  require values of  $f$  that may be in conflict with the constraint (5.15). For  $g' = 0$ ,  $N_{2tot} \sim 2 - 3$ ,  $\sigma_{2i}/m_{Pl} = 0.025$  (the value of this parameter that we use in the next section), and allowing for  $f^2 \sim \frac{1}{4} - \frac{1}{3}$ , a value of  $\sigma_{3i}$  slightly below  $m_{Pl}$  can lead to the required remaining  $\sim 50$  e-foldings. A non-zero value of  $g'$  leads to  $c > 1$  and permits even larger values of  $f$  and, therefore, smaller values of  $\sigma_{3i}$ .

The discussion of the first stage can be carried out in an analogous way, even though the constraints are more complicated. We expect that, similarly to above, there are regions of parameter space for which the primordial spectrum of the first stage is not affected by the presence of the additional fields. Moreover, it is conceivable that several similar inflationary stages generate a total number of e-foldings  $\sim 50$ , in which case the resulting bounds are less stringent. As we have discussed in the introduction and section 2, we have in mind a picture of multiple bursts of inflation, driven by different sectors of the theory, with a sequence of scales starting near  $m_{Pl}$  and continuing down to the scale implied by COBE, or even to lower energy scales. In this work we present only a simplified picture of two of these stages that have direct observational consequences.

Another possibility is that the later stages of inflation are associated with fields that are massive during the first stages or located near the minima of their potential, and, therefore,

do not affect the spectrum. These fields are displaced from their initial position during the reheating and trigger inflation only when the temperature becomes sufficiently low. For such models the constraints discussed above do not apply. The scenario of thermal inflation [40] is a typical example.

The observational consequences of the third inflationary stage are difficult to estimate. One could try to compute the linear mass fluctuation  $\sigma(R)$  for  $R \sim 1 h^{-1}\text{Mpc}$  and compare with the abundance of galaxies at large redshifts [44]. However, the spectrum for the relevant region of  $k$  is strongly affected by the intermediate stage between the second and third inflationary stages, for which a computation is impossible. The fact that the scale  $\mu_3$  is largely unconstrained by previous considerations makes it probable that an agreement with observations is feasible.

## 6 Comparison with observations

In this section we compare the predictions of our model with the experimental data from COBE and the APM galaxy survey. We do not consider the gravitational wave contribution to the spectrum, as we expect it to be small. We also concentrate on the adiabatic scalar contribution given by Eqs. (5.10)–(5.13). We do not consider any early ionization scenarios or HDM. We are interested in examining whether the COBE-DMR measurements can be made compatible with the data of galaxy surveys employing the smallest number of cosmological parameters. More specifically, we consider two cosmological scenarios: 1) A CDM model, with zero cosmological constant, present Hubble parameter  $h = 0.5$  ( $H_0 \equiv h \text{ 100 km/s/Mpc}$ ) and flat geometry  $\Omega_{\text{matter}} = 1$ . We assume that the fraction of the critical density in baryons is  $\Omega_b = 0.05$  and in cold dark matter  $\Omega_{\text{CDM}} = 0.95$ . The helium abundance is  $Y_{\text{He}} = 0.24$ , while we do not consider any massive neutrinos. 2) The same model with  $\Omega_\Lambda = 0.5$ ,  $h = 0.5$ ,  $\Omega_b = 0.05$  and  $\Omega_{\text{CDM}} = 0.45$ .

In both the above scenarios, we use the following parameters for the model of Section 3:  $\lambda_1 = 1$ ,  $\lambda_2 = 0.1$ ,  $g = 7.1 \times 10^{-3}$ ,  $\mu_1/m_{\text{Pl}} = 3.9 \times 10^{-3}$ ,  $\mu_2/m_{\text{Pl}} = 8.8 \times 10^{-4}$ ,  $\sigma_{1i}/m_{\text{Pl}} = 0.36$ ,  $\sigma_{2i}/m_{\text{Pl}} = 0.025$ . For the purpose of this section, the parameters  $M_{1,2}$ , which determine the dimensionalities of the representations of the groups  $\mathcal{M}_{1,2}$  to which the superfields  $\Phi_{1,2}$  belong, can be absorbed in a redefinition of  $\lambda_1$ ,  $\lambda_2$ ,  $g$ . For this reason we set  $M_1 = M_2 = 1$ . For the above choice of parameters the observable part of the first stage of inflation generates  $N_{1\text{tot}} \simeq 5$  e-foldings and a spectrum with a spectral index  $n \simeq 1$ . For the second stage of inflation, Eq. (4.10) predicts  $N_{2\text{tot}} \simeq 2$  e-foldings. However, a more accurate numerical integration of the field evolution equations gives  $N_{2\text{tot}} \simeq 3$ . The spectral index relevant for the scales that cross outside the horizon in the beginning of the second stage of inflation is given by Eq. (5.13) with  $\sigma_2(k) \simeq \sigma_{2i}$  and is  $n \simeq 0.6$ . The intermediate stage affects the scales  $k_2 < k < k_1$  with  $k_1/k_2 \simeq 4.4$  according to Eq. (5.3). The values of the power spectrum for  $k_2$  and  $k_1$  are determined by Eqs. (5.10), (5.11) and satisfy  $P(k_2)/P(k_1) \simeq 11.8$ .

The initial spectrum of fluctuations arising in our model generates matter and radiation perturbations, which, after amplification, give rise to the observed large scale structure and the anisotropies of the cosmic microwave background. In the following, we compare the theoretical predictions of our model with the measured anisotropies of the cosmic microwave background and the observed clustering in the galaxy distribution. For the comparison with the CMB data, we assume a form of the power spectrum in the range  $k_2 < k < k_1$  that interpolates smoothly between the spectrum in the ranges  $k > k_1$  and  $k < k_2$ .

## 6.1 Angular power spectrum of CMB anisotropies

The cosmic microwave background (CMB) radiation, last scattered at the epoch of decoupling, follows a blackbody distribution to high accuracy [45], with a temperature almost independent of direction,  $T = 2.728 \pm 0.002K$ . As it was measured by the DMR experiment on the COBE satellite, the CMB radiation has a tiny variation in intensity at fixed frequency, equivalently expressed as a variation  $\Delta T$  in the temperature:  $\Delta T/T < 10^{-5}$ . The 4-year COBE data is fitted by a scale-free spectrum, with spectral index  $n = 1.2 \pm .3$  and a quadrupole normalization  $Q_{rms} = 15.3_{-2.8}^{+3.7} \mu K$  [46].

In Fig. 2 we compare our theoretical predictions for the angular power spectrum of CMB anisotropies against the most recent CMB flat-band power measurements (we have used the data of Table 1 in Ref. [47]). The coefficients  $C_\ell$  correspond to the expansion of the angular correlation function in powers of the Legendre polynomials  $P_\ell$ . For large  $\ell$ , the angular size (in radians) of a feature in the sky is related to the order of the multipoles that dominate it by  $\ell \sim 1/\theta$ . The angular power spectrum of CMB anisotropies is normalized to the four-year data from COBE-DMR [48]. In order to calculate the predictions of our model for  $C_\ell$  we have used the code CMBFAST of Seljak and Zaldarriaga [38].

In our model, the first stage of inflation leads to a scale-invariant Harrison-Zel'dovich [49] (spectral index  $n = 1$ ) spectrum of perturbations. The intermediate stage and the second stage of inflation affect only the highest multipoles in Fig. 2. For this reason, our prediction for the first acoustic peak in the case  $\Omega_\Lambda = 0$  (short-dashed line) is similar to that of the standard CDM (SCDM) model (solid line) with a Harrison-Zel'dovich spectrum at all scales. Only for multipoles  $l \sim 500$ – $1000$  a drop of the values of  $C_l$  is observed relative to the standard CDM model. This should be contrasted with the double-inflationary model of Refs. [16, 19, 20], which predicts a first acoustic peak that is too low with respect to the Sachs-Wolfe plateau. This problem can be traced to the logarithmic dependence  $\propto \ln^{1/2}(K/k)$  of the spectrum for small  $k$  in this model. Better agreement with the data is obtained for our model with  $\Omega_\Lambda = 0.5$  (long-dashed line).

## 6.2 Angular catalogues of galaxy positions

Angular catalogues of galaxy positions provide strong constraints on theories of structure formation in the universe. In this subsection we compare the predictions of our model with the power spectrum of galaxy clustering derived from the angular APM galaxy survey [30]–[33]. Redshift surveys are more noisy than the APM survey at large scales and subject to more uncertainties due to the distortion of the pattern of galaxy clustering by the peculiar motions of galaxies.

As we have discussed in Section 2, the effects of the non-linear evolution of matter fluctuations (when the density contrast becomes of order 1) must be removed before a comparison is possible with the linear spectrum. This is usually done through  $N$ -body simulations of clustering. Baugh and Gaztañaga [33] have estimated the linear spectrum that gives rise to the APM spectrum for a spatially flat universe with critical density and zero cosmological constant. Their estimate is well fitted by the curve of Eq. (2.1) This result is in agreement with the spectrum obtained through the application of the formula of Jain *et al.* [35] for the relation between the linear and non-linear spectra. The formula of Peacock and Dodds [36] does not lead to very good agreement with the results of the  $N$ -body simulations [34]. The effects of the non-linear evolution are significant for  $k \gtrsim 0.2h\text{Mpc}^{-1}$ .

For the comparison of our predictions with the data, we calculate the transfer function  $T(k)$  to better accuracy than the one provided by Eq. (2.2), by employing the code CMBFAST of Seljak and Zaldarriaga [38]. The linear power spectrum is related to the density perturbation

at horizon crossing through [10]

$$\Delta^2(k) = \frac{k^3 P(k)}{2\pi^2} = \delta_H^2(k) \left(\frac{k}{H_0}\right)^4 T^2(k), \quad (6.1)$$

where the dimensionless quantity  $\Delta^2(k)$  stands for the mass variance per unit interval in  $\ln k$  (i.e.,  $\Delta^2(k) \equiv d\sigma_{mass}^2/d\ln k$ ).

In Fig. 3 we display the power spectrum  $P(k)$  in units of  $(\text{Mpc}/h)^3$  as a function of  $k$  in units of  $h/\text{Mpc}$  for our model with  $\Omega_\Lambda = 0$  and  $k_2 = 0.06 h\text{Mpc}^{-1}$ . For scales  $k < k_2$  the spectral index has been taken  $n = 1$ , while for scales  $k > k_1$  the spectrum is tilted with spectral index  $n = 0.6$ . For scales  $k_2 < k < k_1$  the complicated nature of the intermediate stage makes the calculation of the power spectrum very difficult. The prediction of our model for the linear spectrum is given by the short-dashed line. The points with error bars correspond to the data from the APM angular galaxy catalogue [31, 33]. The fit of Eq. (2.1) for the linear spectrum derived from these data is given by the solid line.

We observe good agreement of our predictions with the linear spectrum expected from the APM data. This agreement should persist for the scales  $k_2 < k < k_1$ , as no strong new feature in the spectrum is expected in this interval (see discussion at the end of Section 5). We point out that we have not assumed any biasing in the galaxy distribution with respect to the underlying mass fluctuations (bias parameter  $b_g = 1$ ). Allowing for other values of  $b_g$  provides an additional degree of freedom that can improve the agreement of our predictions with observations.

The power spectrum for our model with  $\Omega_\Lambda = 0.5$  is given by the long-dashed line in Fig. 4. We compare again with the estimate of Eq. (2.1) for the linear spectrum (solid line). The reason is that for a flat geometry of the universe we do not expect a significant modification of this estimate. The formula of Peacock and Dodds [36] for the relation between the linear and non-linear spectra predicts only a small difference between the spectra for  $\Omega_{matter} = 1$ ,  $\Omega_\Lambda = 0$  and for  $\Omega_{matter} = 0.5$ ,  $\Omega_\Lambda = 0.5$ . We observe a good agreement between our prediction and the linear spectrum in the range  $k \geq 0.26 h\text{Mpc}^{-1}$ . On the other hand, our prediction is significantly above the linear spectrum for  $k \leq 0.06 h\text{Mpc}^{-1}$ . However, the observational data in this last range are dominated by large errors. This makes the estimate for the linear spectrum less accurate.

For values of  $\Omega_\Lambda$  above 0.5, the discrepancy between our prediction and the APM spectrum at large scales is enhanced. Reconciling the prediction with the data can be achieved either through the consideration of a bias parameter different from 1 for the galaxy distribution or a spectral index smaller than 1 for the first stage of inflation.

As a final test of our model, we turn to the calculation of the parameter  $\sigma_8$ , which is a common measure of large-scale clustering. It is defined as the variance of the density field smoothed over a radius  $R = 8 h^{-1}\text{Mpc}$

$$\sigma_8^2 = \frac{1}{H_0^4} \int_0^\infty W^2(kR) \delta_H^2(k) T^2(k) k^3 dk. \quad (6.2)$$

The ‘‘top-hat’’ smoothing function  $W(kR)$  is given by

$$W(kR) = 3 \left[ \frac{\sin(kR)}{(kR)^3} - \frac{\cos(kR)}{(kR)^2} \right]. \quad (6.3)$$

For  $n \sim 0.6$  the largest contribution to the integration of Eq. (6.2) comes from  $k \sim 1/R = 0.125 h\text{Mpc}^{-1}$ . This corresponds to the tilted part of the spectrum near  $k_1$ , for which we have

used  $n = 0.6$  in the calculation of the results presented in Figs. 3 and 4. However, as Fig. 1 indicates, the effective spectral index may be even smaller for  $k$  slightly below  $k_1$ . For this reason we have estimated  $\sigma_8$  allowing for a local variation of  $n$  in the interval  $[0.2, 0.8]$ . We find that  $\sigma_8$  is not very sensitive to the value of  $n$ . Instead, it is determined by the normalization of the spectrum at  $k \simeq k_1$ , which is fixed by  $P(k_2)/P(k_1) \simeq 11.8$  for our choice of parameters of the model. The predicted values of  $\sigma_8$  are near 0.75, both for  $\Omega_\Lambda = 0$  and  $\Omega_\Lambda = 0.5$ . They are in good agreement with the values deduced from the abundances of rich clusters of galaxies:  $\sigma_8 \simeq 0.6 \pm 0.2$  for  $\Omega_{matter} = 1$ ,  $\Omega_\Lambda = 0$  [8], and  $\sigma_8 \simeq 0.85 \pm 0.3$  for  $\Omega_{matter} = 0.5$ ,  $\Omega_\Lambda = 0.5$  [9].

## 7 Summary and conclusions

In this paper we considered the possibility of a multiple-stage inflationary scenario within the context of supersymmetric hybrid inflation. This framework has the nice feature that the observable part of inflation takes place for field values below the Planck scale. This permits the discussion of corrections to the tree-level picture (such as supergravity corrections) in terms of controlled expansions in powers of fields in units of  $m_{Pl}$ . Inflationary models such as the one we considered have been discussed in Ref. [22], and have been shown to survive the supergravity corrections in Ref. [23].

One motivation for the consideration of a scenario with more than one stages of inflation arises from the discrepancy between the inflationary energy scale implied by the COBE data and the Planck scale at which classical general relativity becomes applicable. This discrepancy results in the necessity of an extremely fine-tuned field configuration at the end of the Planck era for the onset of hybrid inflation [26]. The problem can be avoided if inflation takes place in two stages [22]. The first stage has a typical scale  $\sim m_{Pl}$  and occurs naturally. The second has a characteristic scale much below  $m_{Pl}$  and generates the density perturbations that result in the cosmic microwave background anisotropy measured by the DMR experiment on the COBE satellite. It is the logical next step to contemplate the possibility of a multiple-stage inflationary scenario, with a sequence of scales between  $m_{Pl}$  and close or below the one implied by COBE.

Another motivation for the consideration of a multiple-stage scenario stems from the need to reconcile the power spectrum of density perturbations at large scales (obtained through the COBE-DMR measurements for the anisotropies of the cosmic microwave background) with the observed power spectrum at small scales (deduced from galaxy surveys). The standard CDM model with a flat (spectral index  $n = 1$ ) initial spectrum of adiabatic perturbations predicts too much power at small scales, if one normalizes it to the COBE data at large scales. An interesting possibility in order to resolve this discrepancy is to consider power spectra with a break. A strong indication for the location of the break is provided by the form of the power spectrum of galaxy clustering derived from the APM galaxy survey [31, 32, 18, 33]. At  $k_b \simeq 0.05 h \text{ Mpc}^{-1}$  the data support a sharp drop of the spectral index of the primordial spectrum, from a value  $n \simeq 1$  to an average value  $n \sim 0.6$ . This break has been linked to a possible phase transition between two of the inflationary stages in a multiple inflationary scenario [18].

In this paper we presented a model of supersymmetric hybrid inflation that generates a spectrum with a break. As we argued in Section 2, the large deviation of the spectral index from 1 for  $k \lesssim k_b \simeq 0.05 h \text{ Mpc}^{-1}$  results in a small number of e-foldings generated by the stage of inflation relevant for this range of scales. A picture of multiple short bursts of inflation, with significant variations of the spectral index of the primordial spectrum, seems probable.

We computed the spectrum of adiabatic density perturbations for the range of scales that are

relevant for the COBE data and the APM galaxy survey. This requires the explicit discussion of the first two observable stages of inflation, which generate  $\sim 8$  e-foldings. The total number of e-foldings must be  $\sim 60$  for the flatness and horizon problems of standard cosmology to be resolved. However, the stages responsible for the last  $\sim 50$  e-foldings generate density perturbations at scales that are strongly affected by the non-linear evolution. As a result, it is very difficult to extract information on their characteristics.

In our model, the adiabatic density fluctuations during both stages of inflation originate in the quantum fluctuations of the same field. The first stage of inflation generates  $\simeq 5$  e-foldings and a spectrum with index  $n = 1$  for scales  $k \lesssim 0.06 h \text{ Mpc}^{-1}$ . The second stage generates  $\simeq 3$  e-foldings and a spectrum with index  $n \simeq 0.6$  for scales  $k \gtrsim 0.26 h \text{ Mpc}^{-1}$ . The calculation of the spectrum for  $0.06 h \text{ Mpc}^{-1} \lesssim k \lesssim 0.26 h \text{ Mpc}^{-1}$  is prohibited by a very complicated intermediate stage of normal expansion. However, it is probable that no significant new feature arises in this range of scales, as we discussed at the end of Section 5.

We considered two scenarios:

- a) A  $\Lambda$ CDM model, with zero cosmological constant, present Hubble parameter  $h = 0.5 (H_0 \equiv h \text{ 100 km/s/Mpc})$  and flat geometry –  $\Omega_{matter} = 1$ . We assumed that the fraction of the critical density in baryons is  $\Omega_b = 0.05$  and in cold dark matter  $\Omega_{CDM} = 0.95$ .
- b) A scenario with  $\Omega_\Lambda = 0.5$ ,  $\Omega_b = 0.05$  and  $\Omega_{CDM} = 0.45$ .

The comparison of our predictions with observations is given in Figs. 2–4. For the first scenario, the angular power spectrum of CMB anisotropies (Fig. 2) is very similar to the one with a Harrison-Zel’dovich spectrum at all scales. Only for multipoles  $l \sim 500$ – $1000$  a drop of the values of  $C_l$  is observed relative to the standard  $\Lambda$ CDM model. This should be contrasted with the predictions of a model of double chaotic inflation, for which the first Doppler peak is significantly suppressed [20]. The second scenario leads to a better agreement of the generated spectrum with the data. The power spectrum predicted by the first scenario compares well with the linear power spectrum deduced from the APM data (Fig. 3). The agreement is less satisfactory for the second scenario (Fig. 4), even though the discrepancy appears in the region of large data errors. For both scenarios, our predictions for  $\sigma_8$  are in agreement with the values deduced from the abundances of rich clusters of galaxies.

As a closing remark, we point out that the questions of the presence and the nature of a feature in the power spectrum of the galaxy distribution are not settled. Several interpretations and explanations of the data exist (e.g., see Refs. [17, 50]). Our work provides a possible explanation of the observed feature within a multiple-stage inflationary scenario in the context of supersymmetric hybrid inflation.

**Acknowledgements:** It is a pleasure to thank J. Adams, N. Deruelle, E. Gaztañaga, J. Martin, A. Melchiorri, D. Polarski and S. Sarkar for useful discussions, and U. Seljak for help with CMB-FAST. M.S. would also like to thank C.M. Viallet. One of us (M.S.) thanks the Département d’Astrophysique Relativiste et de Cosmologie, Observatory of Paris (Meudon), for hospitality during the preparation of this work. The work of N.T. was supported by the E.C. under TMR contract No. ERBFMRX-CT96-0090.

## References

- [1] P.J. Steinhard, “Cosmology at the Crossroads”, to appear in the *Proceedings of the Snowmass Workshop on Particle Astrophysics and Cosmology*, E. Kolb and R. Peccei, eds. (1995), astro-ph/9502024.
- [2] T.W.B. Kibble, *Phys. Rep.* **67**, 183 (1980).
- [3] R. Crittenden and N. Turok, *Phys. Rev. Lett.* **75**, 2642 (1995); R. Durrer, A. Gangui and M. Sakellariadou, *Phys. Rev. Lett.* **76**, 579 (1996); R. Durrer and M. Sakellariadou, *Phys. Rev. D* **56**, 4480 (1997); R. Durrer, M. Kunz, C. Lineweaver and M. Sakellariadou, *Phys. Rev. Lett.* **79**, 5198 (1997).
- [4] T.S. Bunch and P.C.W. Davies, *Proc. R. Soc. London A* **360**, 117 (1978); A. Vilenkin and L. Ford, *Phys. Rev. D* **26**, 1231 (1982); A.D. Linde, *Phys. Lett. B* **116**, 335 (1982); A. Vilenkin, *Nucl. Phys. B* **226**, 527 (1983).
- [5] S.W. Hawking, *Phys. Lett. B* **115**, 295 (1982); A.H. Guth and S.-Y. Pi, *Phys. Rev. Lett.* **49**, 1110 (1982); D.H. Lyth, *Phys. Lett. B* **147**, 403 (1984); *ibid.* **150**, 465 (1985); *Phys. Rev. D* **31**, 1792 (1985).
- [6] S.D.M. White, C.S. Frenk and M. Davis, *Astrophys. J. Lett.* **274**, L1 (1983); *Astrophys. J.* **287**, 1 (1983).
- [7] M. Davis and P.J.E. Peebles, *Astrophys. J.* **267**, 465 (1983); H.M.P. Couchman and R.G. Carlberg, *Astrophys. J.* **389**, 453 (1992); G. Efstathiou, J.R. Bond and S.D.M. White, *Mon. Not. Roy. Astron. Soc.* **258**, 1 (1992).
- [8] S.D.M. White, G. Efstathiou and C.S. Frenk, *Mon. Not. Roy. Astron. Soc.* **262**, 1023 (1993).
- [9] P.T.P. Viana and A.R. Liddle, *Mon. Not. Roy. Astron. Soc.* **281**, 323 (1996).
- [10] A.R. Liddle and D.H. Lyth, *Phys. Rep.* **231**, 1 (1993).
- [11] R. Cen, N. Gnedin, L. Kofman and J. Ostriker, *Astrophys. J. Lett.* **399**, L11 (1992); F. Adams, J.R. Bond, K. Freese, J. Frieman and A. Olinto, *Phys. Rev. D* **47**, 426 (1993).
- [12] M. White, P.T.P. Viana, A.R. Liddle and D. Scott, *Mon. Not. Roy. Astron. Soc.* **283**, 107 (1996); P.J. Kernan and S. Sarkar, *Phys. Rev. D* **54**, 3681 (1996)
- [13] L.A. Kofman, N.Y. Gnedin and N.A. Bahcall, *Astrophys. J.* **413**, 1 (1983); J.S. Bagla, T. Padmanabhan and J.V. Narlikar, astro-ph/9511102; J.P. Ostriker, and P.J. Steinhardt, *Nature* **377**, 600 (1995).
- [14] N.A. Bahcall, X. Fan and R. Cen, *Astrophys. J. Lett.* **485**, 53 (1997); X. Fan, N.A. Bahcall and R. Cen, *Astrophys. J. Lett.* **490**, 123 (1997); P.M. Garnavich *et al.*, *Astrophys. J. Lett.* **493**, 53 (1998); P.M. Garnavich *et al.*, preprint astro-ph/9806396.
- [15] L.A. Kofman, A.D. Linde and A.A. Starobinsky, *Phys. Lett. B* **157**, 361 (1985); J. Silk and M.S. Turner, *Phys. Rev. D* **35**, 419 (1987).
- [16] D. Polarski and A.A. Starobinsky, *Nucl. Phys. B* **385**, 623 (1992).
- [17] J. Lesgourgues D. Polarski and A.A. Starobinsky, *Mon. Not. Roy. Astron. Soc.* **297**, 769 (1998).
- [18] J.A. Adams, G.G. Ross and S. Sarkar, *Nucl. Phys. B* **503**, 405 (1997).
- [19] P. Peter, D. Polarski and A.A. Starobinsky, *Phys. Rev. D* **50**, 4827 (1994).
- [20] J. Lesgourgues and D. Polarski, *Phys. Rev. D* **56**, 6425 (1997).

- [21] E.J. Copeland, A.R. Liddle, D.H. Lyth, E.D. Stewart and D. Wands, Phys. Rev. D **49**, 6410 (1994); G. Dvali, Q. Shafi and R. Schaefer, Phys. Rev. Lett. **73**, 1886 (1994); E.D. Stewart, Phys. Rev. D **51**, 6847 (1995); G. Lazarides and C. Panagiotakopoulos, Phys. Rev. D **52**, 559 (1995); C. Panagiotakopoulos, Phys. Rev. D **55**, 7335 (1997); Phys. Lett. B **402**, 257 (1997).
- [22] C. Panagiotakopoulos and N. Tetradis, Phys. Rev. D **59**, 083502 (1999).
- [23] G. Lazarides and N. Tetradis, Phys. Rev. D **58**, 123502 (1998).
- [24] G. Lazarides, C. Panagiotakopoulos and N.D. Vlachos, Phys. Rev. D **54**, 1369 (1996).
- [25] G. Lazarides and N.D. Vlachos, Phys. Rev. D **56**, 4562 (1997).
- [26] N. Tetradis, Phys. Rev. D **57**, 5997 (1998).
- [27] A.D. Linde, Phys. Lett. B **259**, 38 (1991); Phys. Rev. D **49**, 748 (1994).
- [28] Z. Berezhiani, D. Comelli and N. Tetradis, Phys. Lett. B **431**, 286 (1998).
- [29] D.H. Lyth, preprint LANCSTH/9614, hep-ph/9609431.
- [30] S.J. Maddox, W.J. Sutherland, G. Efstathiou, L. Loveday and B.A. Peterson, Mon. Not. Roy. Astron. Soc. **243**, 692 (1990); S.J. Maddox, G. Efstathiou and W.J. Sutherland, Mon. Not. Roy. Astron. Soc. **246**, 433 (1990); S.J. Maddox, G. Efstathiou, W.J. Sutherland and L. Loveday, Mon. Not. Roy. Astron. Soc. **283**, 1227 (1996).
- [31] C.M. Baugh and G. Efstathiou, Mon. Not. Roy. Astron. Soc. **265**, 145 (1993).
- [32] J. Peacock, Mon. Not. Roy. Astron. Soc. **284**, 885 (1997).
- [33] E. Gaztañaga and C.M. Baugh, preprint astro-ph/9704246.
- [34] C.M. Baugh and E. Gaztañaga, preprint astro-ph/9601085.
- [35] B. Jain, H.J. Mo and S.D.M. White, Mon. Not. Roy. Astron. Soc. **276**, L25 (1995).
- [36] J.A. Peacock and S.J. Dodds, Mon. Not. Roy. Astron. Soc. **267**, 1020 (1994); **280**, L19 (1996).
- [37] G. Efstathiou, in “The Physics of the Early Universe”, eds. A. Heavens, J. Peacock and A. Davies, SUSSP Publications (1990).
- [38] U. Seljak and M. Zaldarriaga, Astrophys. J. **469**, 7 (1996).
- [39] J.A. Casas and C. Munoz, Phys. Lett. B **216**, 37 (1989); J.A. Casas, J.M. Moreno, C. Munoz and M. Quiros, Nucl. Phys. B **328**, 272 (1989); P. Binétruy and G. Dvali, Phys. Lett. B **388**, 241 (1996); E. Halyo, Phys. Lett. B **387**, 43 (1996).
- [40] D. Lyth and R.D. Stewart, Phys. Rev. Lett. **75**, 201 (1995).
- [41] M. Sasaki and E.D. Stewart, Prog. Theor. Phys. **95**, 71 (1996); J. Garcia-Bellido and D. Wands, Phys. Rev. D **53**, 5437 (1996); **54**, 7181 (1996); D. Wands, Helv. Phys. Acta **69**, 211 (1996).
- [42] V.F. Mukhanov and P.J. Steinhardt, Phys. Lett. B **422**, 52 (1998).
- [43] L.A. Kofman and D.Yu. Pogosyan, Phys. Lett. B **214**, 508 (1988); L. Randall, M. Soljačić and A.H. Guth, Nucl. Phys. B **472**, 377 (1996); J. Garcia-Bellido, A. Linde and D. Wands, Phys. Rev. D **54**, 6040 (1996).
- [44] J.A. Peacock, preprint astro-ph/9805208.
- [45] J.C. Mather, *et al.*, Astrophys. J. Lett. **354**, L37 (1990); E.S. Cheng, *et al.*, Astrophys. J. Lett. **456**, L71 (1996).

- [46] G.F. Smoot, *et al.*, *Astrophys. J.* **396**, L1 (1992); C.L. Bennett, *et al.*, *Astrophys. J.* **464**, L1 (1996).
- [47] C.H. Lineweaver and D. Barbosa, *Astrophys. J.* **496**, 624 (1998).
- [48] E.F. Bunn and M. White, *Astrophys. J.* **480**, 6 (1997).
- [49] H.R. Harrison, *Phys. Rev.* **D1**, 2726 (1970); Y.B. Zel'dovich, *Mon. Not. Roy. Astron. Soc.* **160**, 1 (1972).
- [50] F. Atrio-Barandela, J. Einasto, S. Gottlöber, V. Müller and A. Starobinsky, *JETP Lett.* **66**, 397 (1997).

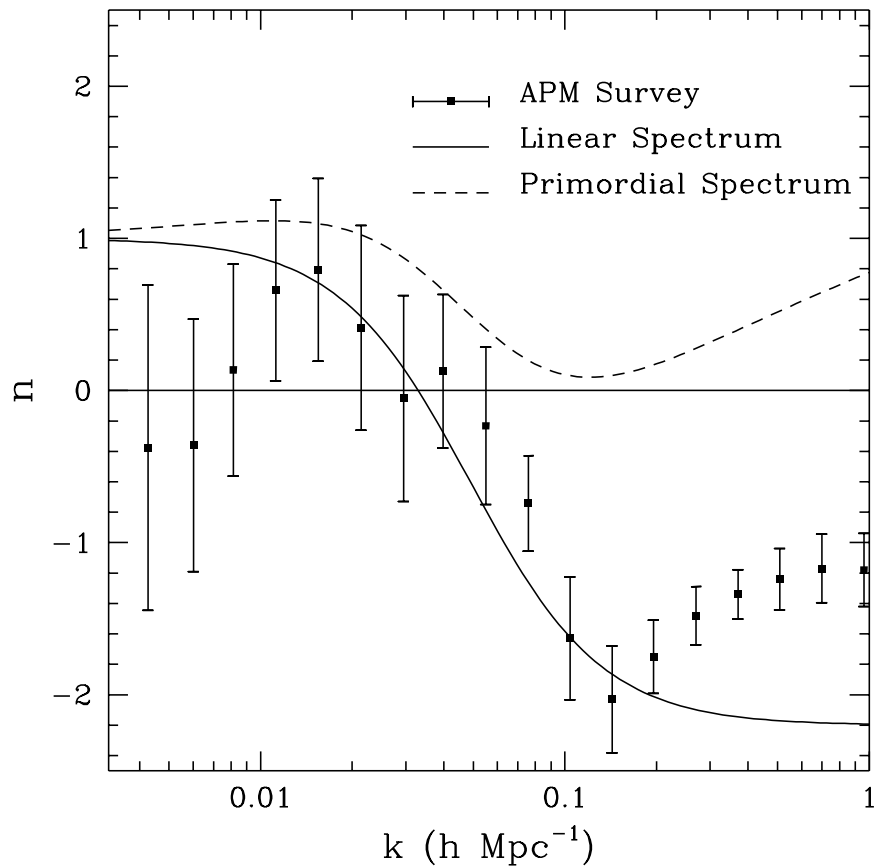


Figure 1: The logarithmic slope of: (a) The power spectrum recovered from the APM angular galaxy catalogue (points with error bars). (b) The estimated linear spectrum that gives rise to the observed spectrum (solid line). (c) The estimated primordial spectrum (dashed line). (After Refs. [18, 33, 34]).

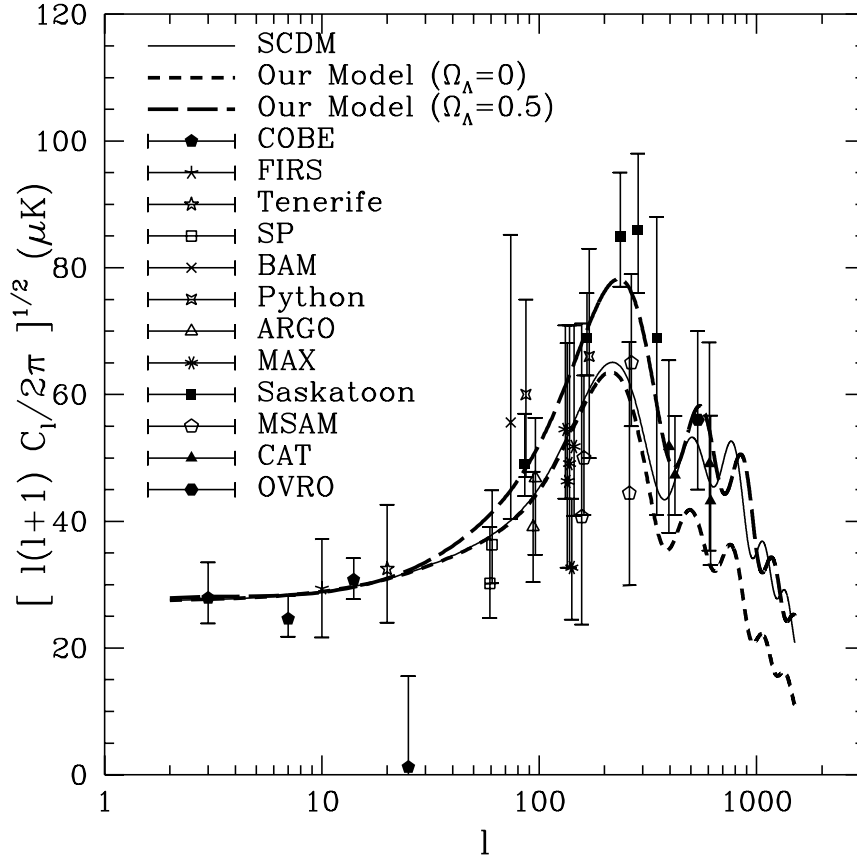


Figure 2: Theoretical predictions for the angular power spectrum of CMB anisotropies in our multiple-stage inflation model, against the most recent CMB flat-band power measurements. We plot  $\sqrt{\ell(\ell+1)C_\ell/(2\pi)}$  in units of  $\mu K$  versus the multipole moment  $\ell$ . The solid line corresponds to the standard CDM model ( $\Omega_\Lambda = 0$ ,  $n = 1$ ). The short-dashed and long-dashed lines correspond to the spectra in our model for  $\Omega_\Lambda = 0$  and  $\Omega_\Lambda = 0.5$  respectively.

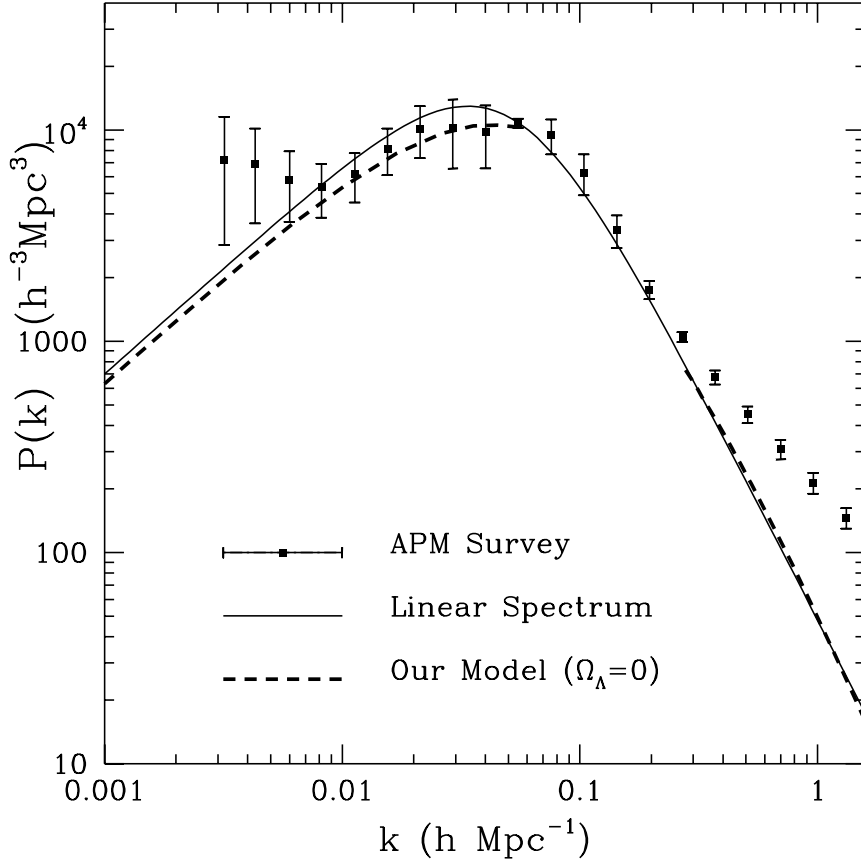


Figure 3: Power spectrum generated in our model (short-dashed line) for  $\Omega_\Lambda = 0$ , plotted together with the APM power spectrum (data points) and the linear spectrum of Eq. (2.1) (solid line). The spectrum is flat for  $k \leq 0.06 \text{ hMpc}^{-1}$  and tilted with  $n = 0.6$  for  $k \geq 0.26 \text{ hMpc}^{-1}$ .

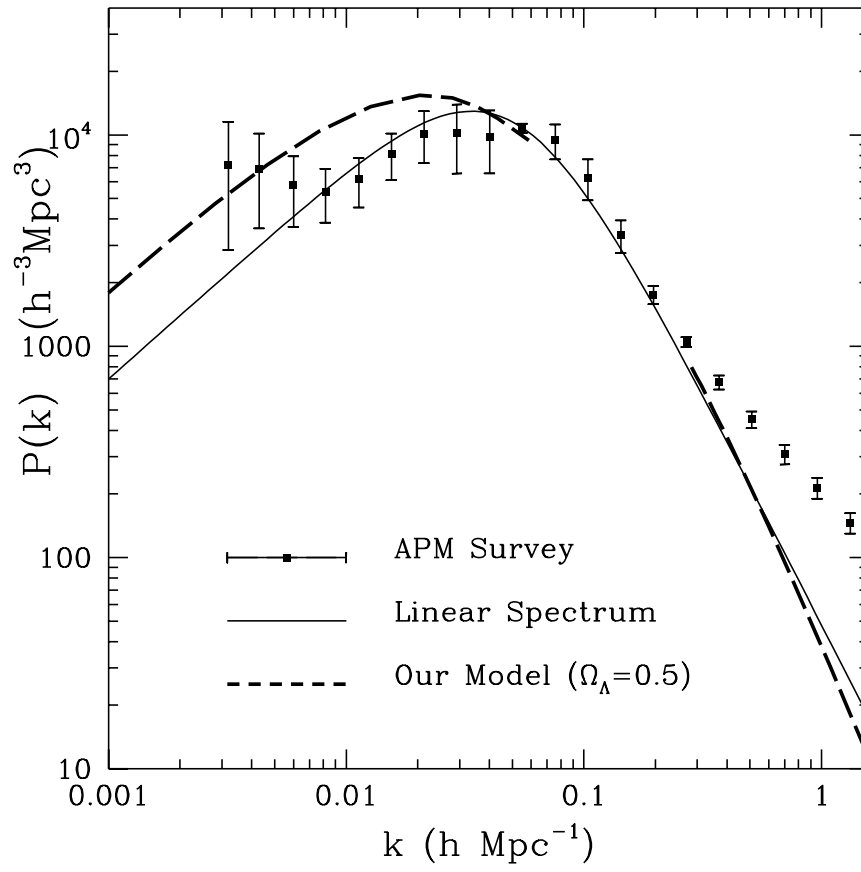


Figure 4: Same as in Fig. 3 for  $\Omega_{\Lambda} = 0.5$ .